J Nanostruct 16(3): 3376-3387, Summer 2026

RESEARCH PAPER

N,O-Chitosan Containing 1,3,4- Thiadiazole/CMC/ Nanoparticles and Study Corrosion Inhibition of Mild Steel

Dhefaf H. Badri, Ruwaidah S. Saeed *, Dheefaf F. Hassan, Huda A. Hassan

Department of Chemistry, College of Education for Pure Science Ibn Al-Haitham, University of Baghdad, Iraq

ARTICLE INFO

Article History:
Received 21 March 2026
Accepted 18 May 2026
Published 01 July 2026

Keywords:
Mild Steel
N, O-Chitosan Containing
Nanoparticles
Thiadiazole

ABSTRACT

Corrosion is a significant chemical and electrochemical process that leads to the degradation of metals through reactions with their environment-including air, moisture, acids, and salts. This occurrence represents a serious industrial and economic issue, causing significant financial losses annually and affecting the soundness of metal structures such as bridges, pipelines, and industrial equipment. In light of the critical need to mitigate corrosion damage, scientific research has prioritized the study of its underlying mechanisms and prevention strategies. Key advancements include the application of corrosion inhibitors, protective coatings, and nanomaterials, all of which have demonstrated significant efficacy in lowering corrosion rates and enhancing the longevity of metallic substrates. In this study, novel nanocomposites were synthesized, beginning with the preparation of 2,5-dimercapto-1,3,4-thiadiazole [1]. This precursor was obtained through the reaction of $NH_2NH_2.H_2O$ (0.01 mol, 99%) with carbon disulfide (0.02 mol). Subsequently, compound [1] was reacted with chloroacetic acid and anhydrous sodium carbonate in distilled water to yield 2,2'-((1,3,4-thiadiazole-2,5-diyl)bis(sulfanediyl))diacetic acid [2]. To prepare the corresponding acid chloride, compound [2] was treated with thionyl chloride in benzene to produce compound [3]. Finally, the O-chitosan derivative [4] was synthesized via the esterification of chitosan with compound [3] in an acidic aqueous medium, following the Fischer esterification method. O,N-carboxymethyl chitosan [5] was synthesized via the reaction of chitosan with compound [4] in a mixture of chloroform and pyridine. Subsequently, the modified chitosan derivatives [4, 5] were blended with carboxymethyl cellulose (CMC) to yield polymer blends [6, 7]. These blends were further incorporated with copper, silver, or zinc nanoparticles using a hotplate stirrer for three hours to produce nanocomposites [8–13]. The structural and morphological characteristics of the synthesized polymers and composites were characterized using (FTIR), (^{1}H-NMR), Field Emission Scanning Electron Microscopy (FESEM), and Transmission Electron Microscopy (TEM). Testing the corrosion inhibition of modified CS, modified CS /CMC and nanocomposites on mild steel in 0.1M HCl was conducted by weight loss analysis and electrochemical measurements were used to explore the corrosion inhibition study. The results show that nanocomposites [11-13] have a higher inhibition rate than blended polymer [7], modified CS[5] against the corrosion of carbon steel.

How to cite this article
H. Badri D., S. Saeed R., F. Hassan D., A. Hassan H. N,O-Chitosan Containing 1,3,4- Thiadiazole/CMC/ Nanoparticles and Study Corrosion Inhibition of Mild Steel . J Nanostruct, 2026; 16(3):3376-3387. DOI: 10.22052/JNS.2026.03.031

* *Corresponding Author Email: ruaida.s.s@ihcoedu.uobaghdad.edu.iq*

INTRODUCTION

Corrosion represents a critical challenge within the industrial sector, resulting in profound economic consequences. These losses primarily stem from the degradation of material structural integrity, which necessitates extensive restoration efforts and frequently causes maintenance expenditures to exceed initial budgetary projections [1]. To mitigate these effects, techniques such as cathodic protection and the use of inhibitors are frequently implemented. Since eliminating corrosion entirely is often impossible, the focus shifts toward the more practical goal of controlling and reducing its rate [2-4]. One of the most cost-effective and accessible methods for corrosion mitigation involves the addition of inhibitors to the substrate's environment. Inhibitors are chemical compounds that, when introduced in low concentrations to the electrolyte, significantly reduce the corrosion rate by interfering with the electrochemical kinetics of the system [5]. Corrosion is characterized as the deterioration of metallic elements and their alloys through electrochemical interactions with thier environment. This process occurs due to the inherent tendency of metals to revert to their thermodynamically stable mineral forms [6,7]. While unavoidable, corrosion can be managed through various preventive measures, including: cathodic protection, anodic protection, coating, alloying and using inhibitors, etc[8]. Out of these methods, inhibitors are highly effective as they reduce the aggressiveness of the corrosive aqueous environments by creating a protective molecular film on the metal surface [8]. Recent studies highlight chitosan as an effective inhibitor solution in acidic environments, particularly for protecting low-carbon steel. The efficiency of chitosan typically improves as its concentration increases, up to a specific optimal threshold [9-11]. Chitosan (CS), is a naturally occurring polycationic linear polysaccharide that is derived from the chitin, is a copolymer made up of N-acetylglucosamine and glucosamine [12-14]. Chitosan (CS) is a naturally occurring, positively charged linear polysaccharide produced from chitin. It functions as a copolymer composed of N-acetyl-D-glucosamine and D-glucosamine units. Following cellulose, chitin is the most prevalent natural polymer on Earth, acting as a fundamental structural component in the outer shells of crustaceans (including shrimp and crabs), as well as in insects and the cell walls of fungi [15-18].

Chitosan (CS) is extensively acknowledged for its biocompatibility, biodegradability, and non-toxic profile, making it a highly secure material. Its biological profile encompasses antimalignant, antitumor, and antimicrobial capabilities, and it is regularly utilized as a blood thinner within pharmaceutical applications [19-22]. The existence of hydroxyl (-OH) and amino ($-NH_2$) functional groups within the structure of CS [23] allows for its easy conversion into a diverse array of functionalized derivatives [24-28]. 1,3,4-Thiadiazole derivatives play significant roles as scaffolds for corrosion inhibition owing to the chemical nature of groups such as C=N, C-S, amine, and N-N linkages. Furthermore, the thiadiazole ring possesses π -electrons, which allow it to bond easily to the surface of mild steel (MS), thereby reducing the corrosion rate [29]. Consequently, chitosan has been modified with 1,3,4-thiadiazole compounds to create derivatives with enhanced solubility, biocompatibility, biological activity, and hydrophilicity [30-32]. Carboxymethyl cellulose (CMC) is a water-soluble, negatively charged derivative of cellulose. Cellulose itself is a long-chain polymer consisting of anhydro-glucose units [33]. CMC exhibits excellent biocompatibility, leading to its widespread use in cleaning products, cosmeceuticals, pharmaceuticals, textiles, paper, adhesives, ceramics, and the food industry [33]. CMC exhibits excellent biocompatibility, making it widely used in cleaning products, cosmeceuticals, medicines, paper, textiles, adhesives, ceramics, food and pharmaceutical industries [34]. The presence of two types of reactive sites (carboxyl and hydroxyl) within its structure, combined with its high water solubility, enhances its chemical reactivity and facilitates numerous further modifications [35-38]. CMC is a linear polymer that exists as a colorless, fragrance-free, non-toxic, water-soluble powder and a highly transparent gel. Soluble in mild alkaline solutions, exhibiting superior dispersion and binding properties [39]. CMC has environmentally beneficial characteristics, including safety, biodegradability, biocompatibility, non-toxicity, and environmental sensitivity. The availability of CMC would facilitate its entry into the pharmaceutical, clinical, and food industries [40,41]. CMC chains can interact with oppositely charged polyelectrolytes, such as chitosan, to form three-dimensional hydrogel networks. It has been effectively utilized as an anticorrosive agent for low-carbon steel in

aqueous media [42]. For example, Rajendran et al. examined the corrosion patterns of carbon steel in the presence of a carboxymethyl cellulose (CMC) and 1-hydroxyethane-1,1-diphosphonic acid (HEDP) system; their findings underscore that the application of polymers and their derivatives as sustainable 'green' corrosion inhibitors for metals and alloys remains a significant area of research [43].

MATERIALS AND METHODS

Materials

Powder of Copper oxide Nano (CuONPs, size 40nm), Silver Nano(AgNPs, size 20nm) and Zinc oxide (ZnONPs, size 10-30nm) by US, Research Nanomaterils, Inc. All Chemicals were provided by BDH, SCR and CDH.

Instrumentation

(FT-IR) spectra were recorded using a Shimadzu FTIR-8400S spectrometer over a spectral range of 400–4000 cm^{-1}. The ^{1}HNMR spectra were obtained using an Ultra Shield 400 MHz spectrometer from Bruker, University of Tehran, Iran. TMS was employed as an internal standard with DMSO serving as the solvent. Field Emission scanning Electron Microscopy (FESEM) and Transmission Electron Microscopy (TEM) were conducted at the University of Tehran, Iran.

Methods of Synthesis

Synthesis of 2,5-dimercapto-1,3,4-Thiadiazole [1] [44]

A mixture of 99% $NH_2NH_2.H_2O$ (5 mL, 0.10 mol) and CS_2 (1.2 mL, 0.02 mol) in dry pyridine (50 mL) was refluxed for 5 hours. Following the reaction, the excess solvent was removed under reduced pressure via distillation. The resulting solid was precipitated by the addition of water (25 mL) and concentrated HCL (5 mL). The crude product was collected by filtration and purified via recrystallization from ethanol.

Synthesis of Compound[2] [45]

An aliquot of 2,5-dimercapto-1,3,4-thiadiazole [1] (0.01mol) was combined with anhydrous sodium carbonate (0.04mol) in (15ml) of distilled water. Following this, chloroacetic acid (0.01mol) was added to the mixture. The resulting solution was heated under reflux for 6 hours. Upon completion, the mixture was acidified to pH 2 using concentrated hydrochloric acid to precipitate the product. The crude solid was isolated via filtration, washed thoroughly with distilled water, and purified by recrystallization from absolute ethanol to yield compound [2].

Synthesis of Compound [3] [46]

A solution of compound [3] (0.01mol) and thionyl chloride (0.02 mol) in 15 ml of anhydrous benzene was heated at reflux for 8 hours. Following the completion of the reaction, the solvent and residual thionyl chloride were removed under reduced pressure to yield the crude product.

Synthesis of O- Chitosan derivatives [4] [47]

Chitosan (0.5 g) was suspended in 25 mL of 2M H_2SO_4, followed by the addition of 0.01 mol of compound [2]. The mixture was heated under reflux for eight hours and then allowed to cool to room temperature. The solution was neutralized to pH 7 using $NaHCO_3$. The resulting product was precipitated in acetone, collected via filtration, and washed thoroughly with additional acetone to remove any residual acid. Finally, the product was dried in an oven at 60°C for 24 hours.

Synthesis of O,N Chitosan derivatives [5] [48]

Initially, 0.5 g of chitosan was immersed in a 50 mL mixture of chloroform and pyridine (1:1 ratio) for duration of 10 hours. Subsequently, compound [3] was added to the mixture while maintained in an ice-water bath. The resulting solution was subjected to continuous stirring at 100°C for 14 hours.

Following this period, the mixture was allowed to cool and was then poured into 25 mL of methanol. After being further chilled to 4°C, The resulting solution underwent filtration, after which the collected precipitate was washed extensively with methanol and subsequently dried at 50°C.

Synthesis of Polymers Blend [6,7] [49]

Polymer blends were prepared using the solvent casting method. The modified chitosan (CS) solution was prepared by dissolving the polymer in 2% (v/v) aqueous acetic acid under constant stirring at ambient temperature. Simultaneously, carboxymethyl cellulose (CMC) was dissolved in distilled water to achieve a 5 wt% concentration. The two solutions were then combined and homogenized using stirrering for 60 minutes. The modified CS/CMC blends were synthesized at a weight ratio of 5:5.

Synthesis of Modified CS/ CMC/Nanocomposites [8-13] [50]

A 100 mg sample of the dried, modified CS/ CMC blend [6, 7] was immersed in 50 mL of a CuO, Ag, or ZnO solution (250 mg/L). The mixture was agitated using a hotplate stirrer for 3 hours to facilitate the bonding of the copper, silver, or zinc nanometals within the blend matrix [26].

RESULTS AND DISCUSSION

The synthesis of new nanocomposites beginning with 2,5-dimercapto-1,3,4-Thiadiazole [1] is demonstrated in Fig. 1. Compound [1] have been created by reacting hydrazine hydrate (99%) with 2mol of carbon disulfide in dry pyridine. The compound's FT-IR [1] revealed appearance bands at (2547) and (1639) cm^{-1} respectively, owing to SH group and (C=N).

Compound [2] was synthesized under basic conditions via the reaction of compound [1] with chloroacetic acid in distilled water. The FTIR spectrum of [2] confirmed the formation of the product, displaying a characteristic broad absorption band between 3400–2400 cm^{-1} (O-H stretch) and a sharp band at 1684 cm^{-1} corresponding to the carboxylic carbonyl group

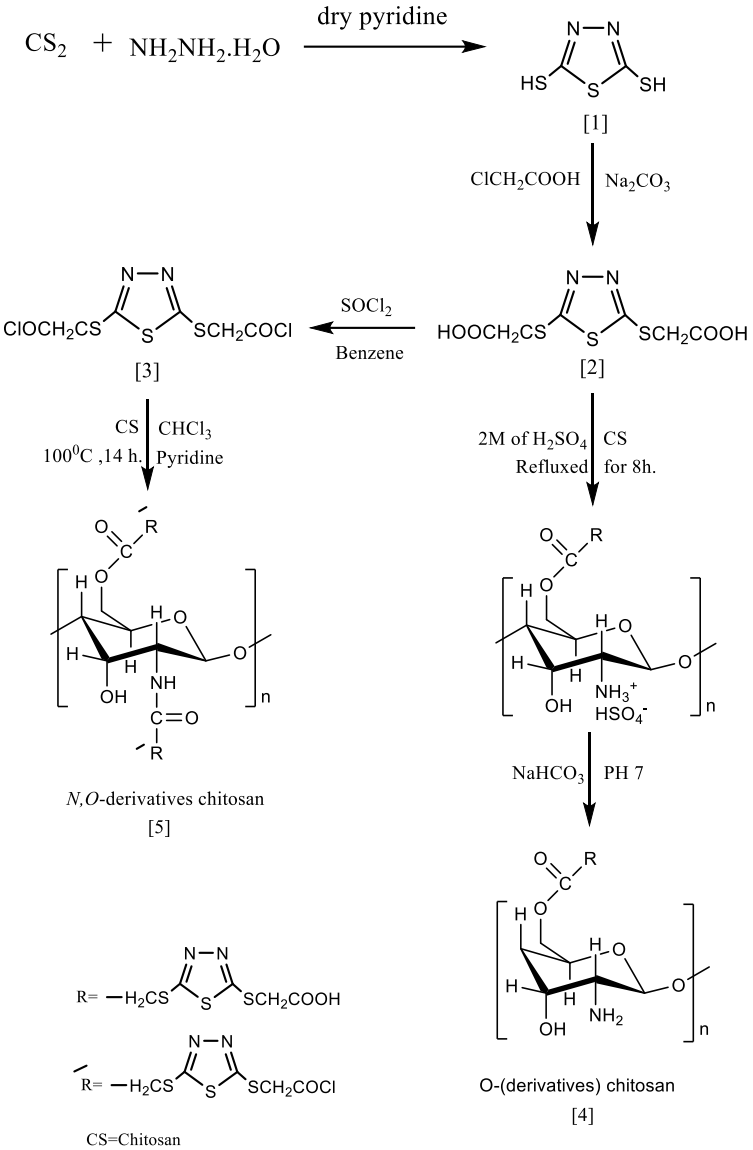

Fig. 1. The synthetic route for target derivatives [1-5].

(C=O).

The ^{1}H-NMR spectrums further supported the structure, exhibiting a broad singlet signal wth chemical shift at δ 12.07 ppm integrating for two protons, assigned to the carboxylic acid groups. Additionally, a signal appeared at δ 4.35 ppm attributed to two protons of SH group. Compound [2] reacted with thionyl chloride in dry benzene to product compound [3]. The FTIR spectrum of compound [3] confirmed the absence of the characteristic carboxylic acid bands at (1684) cm^{-1} (C=O) and (3400-2500) cm^{-1}(O-H). Instead, a new absorption band appeared at 1737cm^{-1}, corresponding to the carbonyl group of the acyl chloride. O-chitosan derivatives [4] produced through the reaction between compound [2] and chitosan in distilled water in acidic media. The presence of O-H and N-H groups in polymer [4] was confirmed by a strong, broad signal at 3294 cm^{-1} in its FT-IR spectrum. This broadening confirms the presence of extensive intra- and intermolecular hydrogen bonding within the chitosan framework. Additionally, a new absorption band appeared at 1714 cm^{-1}, corresponding to the C=O stretching vibration of the ester group.

O,N-chitosan derivatives [5] were synthesized

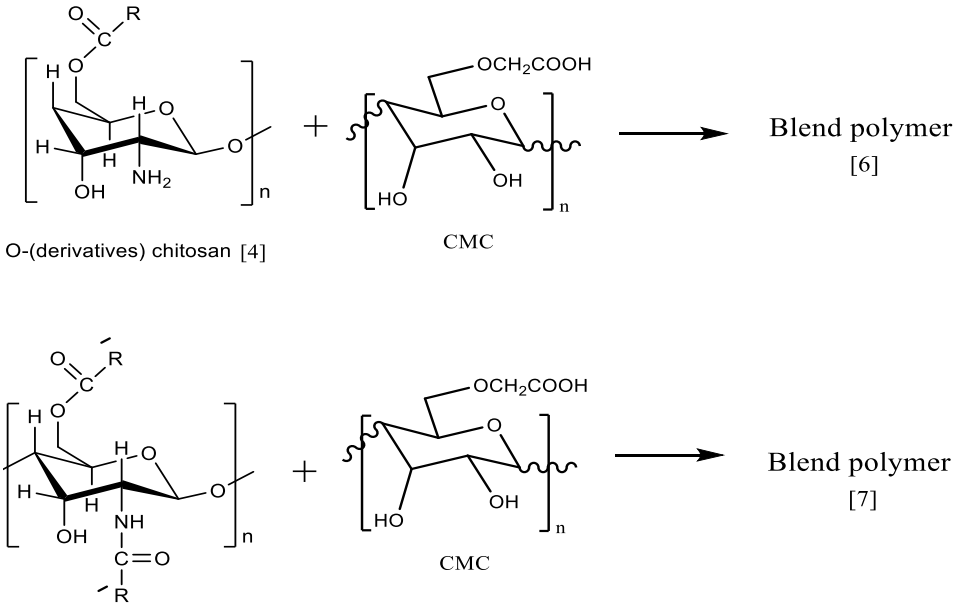

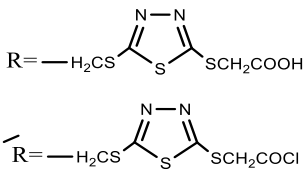

Fig. 2. Synthesis of blend polymers [6,7].

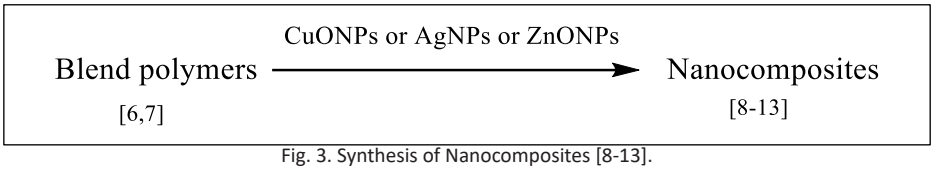

Fig. 3. Synthesis of Nanocomposites [8-13].

via the reaction of [3] with chitosan, utilizing a mixture of pyridine and trichloromethane as the solvent system.The FT-IR spectrum of polymer [5] exhibited a broad absorption band at 3365 cm^{-1}, attributed to the N-H and O-H stretching vibrations involved in intra- and intermolecular hydrogen bonding within the chitosan framework. The successful formation of the derivative was further confirmed by the emergence of new characteristic bands at 1740 $cm^{-1}$and 1678 cm^{-1}, corresponding to the carbonyl groups (C=O) of the ester and amide functionalities, respectively.

In the ^{1}H NMR spectrum of polymer [5], a distinct singlet signal appeared at δ 9.66 ppm, which is assigned to the protons of the NHC=O group. Additionally, a singlet signal at δ 4.87 ppm was observed, corresponding to the hydroxyl OH protons of the chitosan, 3.04 - 3.75 (s,H-1, H-3, H-4, H-5, and H-6 the non-anomeric proton of chitosan), singlet signal at δ (5.31-5.94) ppm for eight proton of SCH_2 groups. By casting method, blend polymers [6,7] are made from modified CS[4,5] with CMC, as revealed by FT-IR data. The band broadening in the 2400-3600 cm^{-1} region indicates strong intermolecular hydrogen bonding between the amino groups of CS and the hydroxyl groups of CMC. Additionally, a peak at 1632 cm^{-1} corresponds to the C=N bond, while a peak at

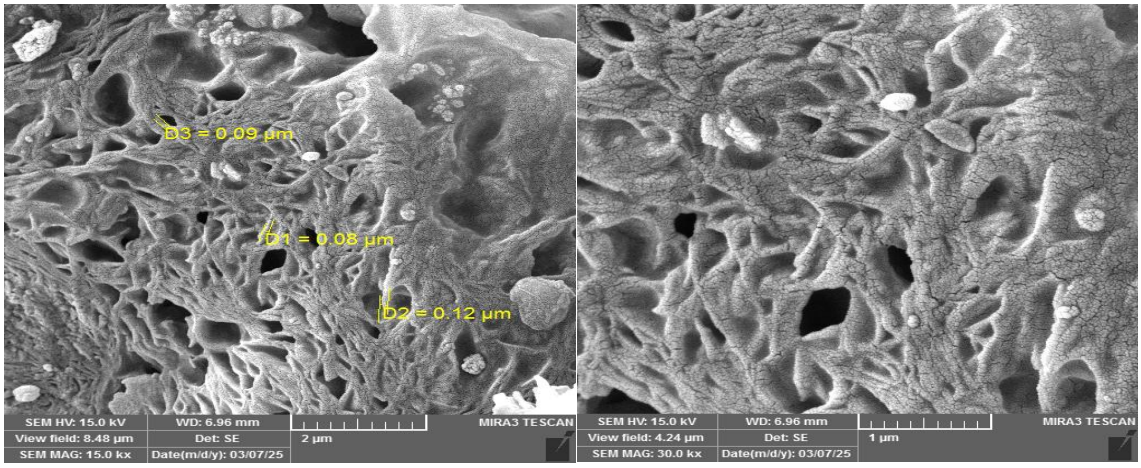

Fig. 4. FESEM of blend polymer [7].

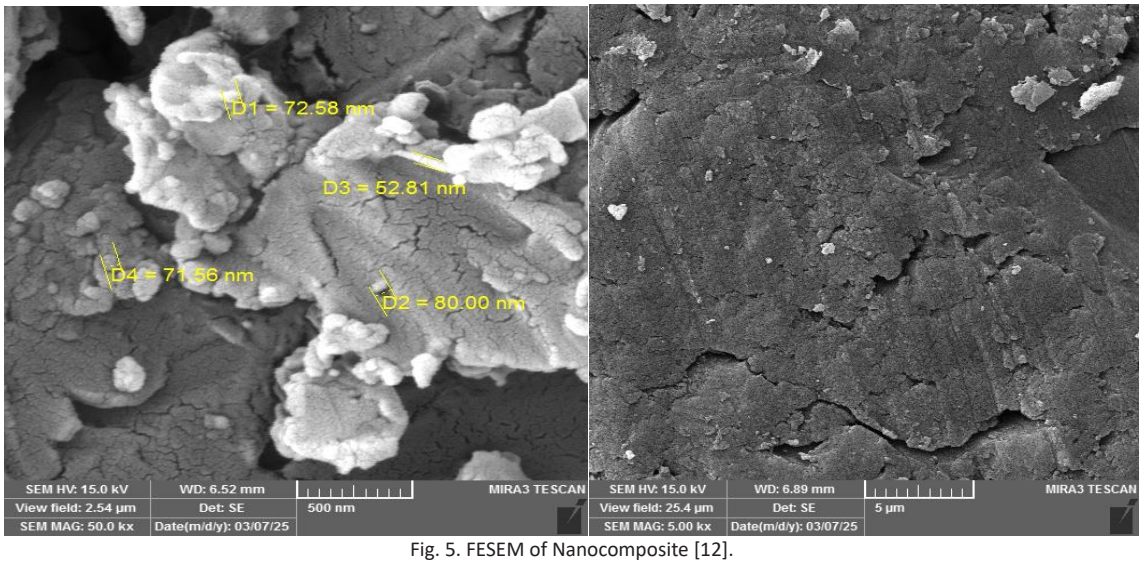

Fig. 5. FESEM of Nanocomposite [12].

(1710) cm^{-1} is attributed to the carbonyl of the ester. By stirring alone, the synthesis of nanocomposites [8-13] based on CuO, Ag, or ZnO nanoparticles (NPs) combined with polymer blends [6,7] exhibits characteristic peaks at (3189) cm^{-1}. These peaks reveal O-H stretching from intramolecular and intermolecular hydrogen bonds. Additionally, shifting is observed in the asymmetric and symmetric C-H stretching vibrations of alkyl groups at (2889,2960) cm^{-1}, while peaks between 400 and 800 cm^{-1} indicate metal-oxide bonding (Cu, Ag, Zn), which confirms the successful formation of the nanoparticles.

FESEM Studies

FESEM micrographs have been utilized to study changes in surface morphology for prepared blend polymer[7] and nanocomposites [12],[13] as shown in Figs. 4-7, respectively. In FESEM images, blend polymer the pores' average pore size is compared to the nanocomposites pore size, the size of the pores in the blend polymer was (0.08-0.12) um, while the size of the pores in the nanocomposites was (52-80), (32-63) nm. After the nanoparticles-to-blend polymer interaction, the FESEM images showed that the surface of the produced blends had undergone considerable changes, as we observed a homogeneous distribution of polymers on the surface of the polymer blend. It was observed that the AgNPs and ZnONPs have homogeneous distributions on the surface of the matrix[50].

Transmission Electron Microscopy (TEM)

The AgNPs are well dispersed and have a semi-spherical morphology, according to the TEM

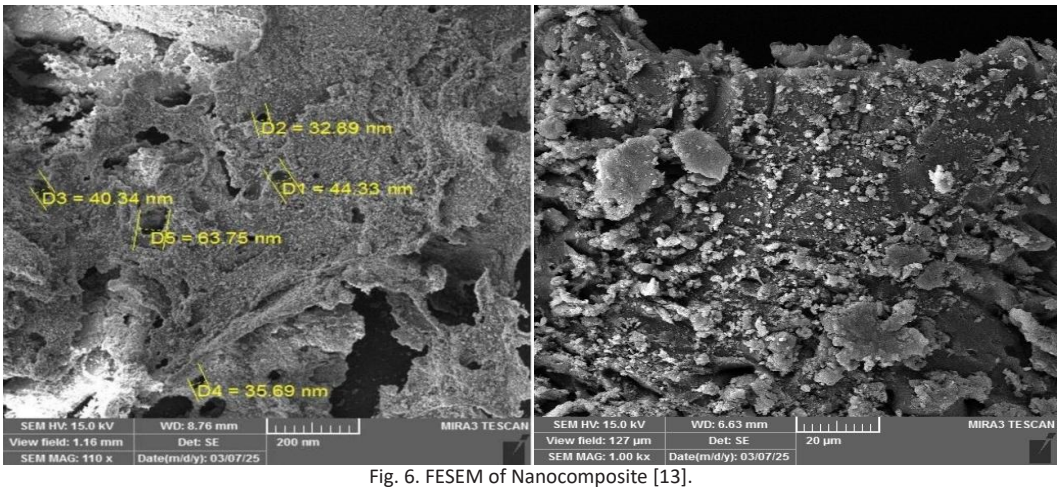

Fig. 6. FESEM of Nanocomposite [13].

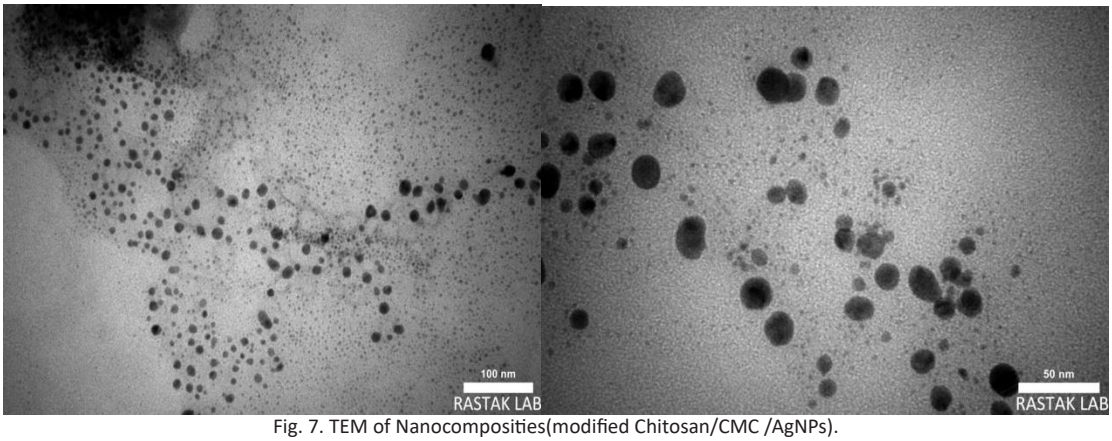

Fig. 7. TEM of Nanocomposities(modified Chitosan/CMC /AgNPs).

image of the modified chitosan/CMC suspension drop-cast with AgNPs. Although the particles are oriented differently and are closed, there are no signs of agglomeration and had sizes in the range of (5-50) nm, Fig. 7. The particles appeared spherical, with a thin layer of silver around modified CS/CMC. As a result, the produced AgNps in modified chitosan/CMC are more stable. The modified chitosan /CMC appeared to be coated with a layer of silver particles validating the generation of CS/CMC/AgNPs [50].

Corrosion inhibition [51]

The chemical composition of carbon steel samples is as follows: C, 0.22; Fe, 99.20; Cu, 0.19; Si, 0.28; Mn, 0.03; Ca, 0.02; and S, 0.06. Possibly the most widely used method for assessing inhibition is the gravimetric approach, which measures weight loss. The weight-loss method has demonstrated such simplicity and reliability that it is now the established baseline for measurement in several scheduled corrosion monitoring programs. Weight-loss measurements were conducted using 250 ml beakers containing 100 ml of the test solution at room temperature. The iron coupons were weighed and then fully submerged in the beakers, suspended from a rod by a hook. After being immersed for seven hours, the coupons were rinsed with distilled water, dried, and reweighed. The difference in weight before and after immersion in the various testing solutions was then used to calculate the total weight loss, expressed in grams.

Table 1 shows Inhibition effectiveness of polymers and nanocomposites.

$$\mathrm{I.E} = \frac{\mathrm{Wu} - \mathrm{Wi}}{\mathrm{Wu}} \times 100 \quad (1)$$

I.E. represents the inhibitor solution's inhibition efficiency.

Wi is the weight loss in the inhibitor solution, and Wu is the weight loss in the control solution.

Modified CS[5], modified CS/CMC[7], modified CS/CMC/CuONPs[11], modified CS/CMC/AgNPs[12], modified CS/CMC/ZnONPs[13] demonstrated a high degree of corrosion inhibition against carbon steel corrosion in an acidic medium. This can be attributed to the presence of p electrons in aromatic systems, multiple bonds, and the electronegative atom (N) in inhibitor molecule structures. This group has an inductive effect that makes the aromatic ring more active and boosts electron density. These modifications can make it much easier for the inhibitor to absorb, which boosts both protection and absorption. The study indicates that compounds that adhere to the metal surface work

Table 1. Inhibition effectiveness of polymers and nanocomposites in 0.1M HCl solutions at different concentrations of all compounds at room temperature.

Beaker No.	Compound	Concentration	Initial Weight	Final Weight	Loss of weight	% Loss in weight	I.E. (%)
1	Control [HCl]	0.1M	5.913	4.177	1.736	29.359	-
2	HCl+ modified CS [5]	50 ppm	5.782	4.901	0.881	15.236	49.251
3	HCl+ modified CS[5]	100 ppm	5.812	4.978	0.834	14.349	51.958
4	HCl+ modified CS/CMC[7]	50 ppm	6.265	5.608	0.657	10.486	64.283
5	HCl+ modified CS/CMC[7]	100 ppm	6.112	5.545	0.567	9.276	67.338
6	HCl+ modified CS/CMC/CuONPs[11]	50 ppm	6.301	5.88	0.421	6.681	75.748
7	HCl+ modified CS/CMC/CuONPs[11]	100ppm	5.911	5.61	0.301	5.092	82.661
8	HCl + modified CS/CMC/AgNPs[12]	50ppm	5.991	5.849	0.142	2.470	91.820
9	HCl + modified CS/CMC/AgNPs[12]	100ppm	6.012	5.881	0.131	2.178	92.453
10	HCl+ modified CS/CMC/ ZnONPs[13]	50ppm	5.667	5.457	0.210	3.705	87.903
11	HCl+ modified CS/CMC/ZnONPs[13]	100ppm	5.545	5.354	0.191	3.444	88.997

as adsorption inhibitors and stop corrosion. It is important to note that nanoparticles, along with Chitosan (CS) and Carboxymethyl Cellulose (CMC) compounds, can significantly enhance corrosion protection by forming a thin, passive layer on a material's surface. This defensive membrane precludes the contact of degradative chemicals with the metal base. Specifically, this method works by either inhibiting the redox (reduction-oxidation) processes within the corrosion system or by neutralizing the effects of dissolved oxygen. Furthermore, the integration of Copper (Cu), Silver (Ag), and Zinc (Zn) nanoparticles helps stabilize the formation of these protective layers, effectively shielding metal surfaces against environmental degradation [52].

Mechanism of Corrosion Inhibition

Chemical adsorption of inhibitor molecules is facilitated by the electron-accepting nature of the unoccupied d-orbitals in iron (Fe) atoms. Specifically, coordinate bonds are formed through the overlap of the vacant 3d-orbitals of Fe with the p-orbital lone pair of the inhibitor.

The presence of additional hydroxyl substitution groups on the aromatic ring further enhances this process. The inductive effect of these groups increases the electron density and activates the aromatic ring, leading to more efficient adsorption and improved corrosion protection. This indicates that these substances function as effective adsorptive inhibitors by adhering strongly to the metal surface. Furthermore, the substantial

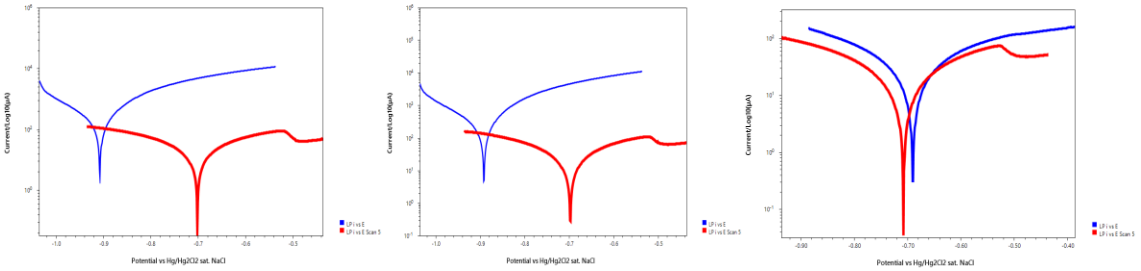

Fig. 8. Polarization curves for corrosion of blank (blue curve) and nanocomposite [8] (red curve) at 298K,308K,318K respectively.

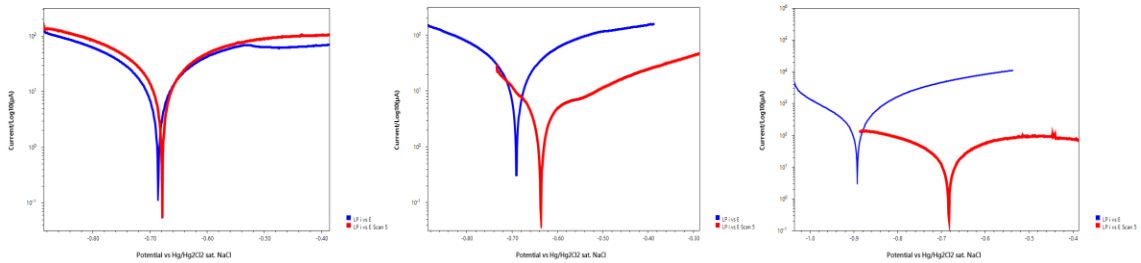

Fig. 9. Polarization curves for corrosion of blank (blue curve) and nanocomposite [9] (red curve) at 298K,308K,318K respectively.

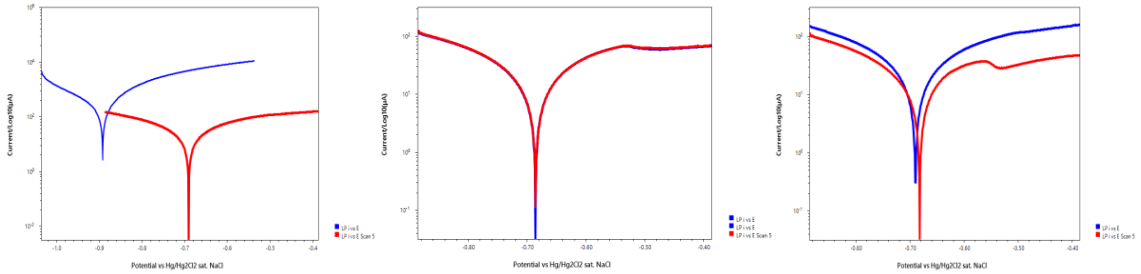

Fig. 10. Polarization curves for corrosion of blank (blue curve) and nanocomposite [10] (red curve) at 298K,308K,318K respectively.

Table 2. Corrosion parameters for blank and compound in HCl solutions.

Inhibitor Concentration	T (K)	-Ecorr (mV)	Icorr (mA/cm²)	βc (mV/dec)	βa (mV/dec)	PL (mm/y)	Rp (Ω/cm²)	$PE\%$
Blank	318	672	0.29000	107	81	1.423	145.5	
	308	674	0.30300	108	87	1.487	138.1	
	298	656	0.39830	128	96	1.955	119.7	
ModifiedCS/CMC/ CuONPs[11]	298	472	0.05145	365	374	0.253	3117	82.25
	308	455	0.08131	513	600	0.399	2953	73.16
	318	461	0.08815	395	411	0.433	1986	77.86
ModifiedCS/CMC/ AgNPs[12]	298	449	0.04981	274	397	0.244	2826	87.49
	308	441	0.05611	264	313	0.275	2219	81.48
	318	447	0.05838	262	321	0.287	2146	85.34
Modified CS/CMC/ ZnONPs[13]	298	447	0.04140	278	487	0.203	3716	85.72
	308	448	0.04186	254	284	0.205	2781	86.18
	318	453	0.05303	244	259	0.260	2056	86.68

E corrosion, I corrosion, Ma, I corrosion per surface area, A/cm², Rp Polarization Resistance, Ω, βa Anodic Tafel constant, V/decade, βc Cathodic, Tafel constant, V/decade, CR Corrosion rate, mm/year, IE% inhibition efficiency

molecular size and high molecular weight of these compounds and nanoparticles contribute to their superior inhibition efficiency [53].

Corrosion / EIS measurement [54]

The Corrosion/EIS measurement setup consists of a host computer, a thermostat, and a magnetic stirrer, interfaced with a Vertex. One Potentiostat/Galvanostat/EIS (Ivium Technologies, Netherlands). The electrochemical cell is a double-walled Pyrex glass cell (100 mL capacity) featuring internal and external bowls for temperature control. Measurements were performed using a standardized three-electrode cell:

Working Electrode (WE): Carbon steel, used to determine the electrochemical potential.

Counter (Auxiliary) Electrode (CE): A platinum electrode with a surface area of 1 cm².

Reference Electrode (RE): A Saturated Calomel Electrode (SCE, Hg/Hg_2Cl_2in sat. KCl) as reference electrode.

Before measurements, the working electrode was immersed in the test solution for 15 minutes to achieve a steady-state Open Circuit Potential (Eocp). All experiments were conducted at 298, 308, and 318 K using a cooling-heating circulating water bath to maintain precise thermal control.

Polarization Curves [55,56]

Corrosion characteristics were evaluated based on the experimental data. The corrosion potential (Ecorr) and corrosion current density (Icorr) were derived by extrapolating the anodic and cathodic Tafel slopes in a 0.1M HCl medium, both with and without the addition of inhibitor molecules. Additionally, the Tafel constants for the anodic (ba) and cathodic (bc) regions were determined. Table 2 presents the results for the Tafel slopes (mV/dec), corrosion potential Ecorr (mV), corrosion current density ICD (A/cm²), and protection efficiency PE:

$$\%\mathrm{IE} = \frac{(\mathrm{icorr})\mathrm{o} - (\mathrm{icorr})}{(\mathrm{icorr})\mathrm{o}} \times 100 \qquad (2)$$

Where (icorr) o is the corrosion current density in the absence of inhibitors, and (icorr) is the corrosion current density in the presence of inhibitors.

CONCLUSION

The goal of this study is to create new nanocomposites through a sequence of reactions. This process involves synthesizing new compounds, grafting them onto chitosan, blending the modified polymers with carboxymethyl cellulose (CMC), and finally coating the resulting polymer matrix with various nanoparticles. The structural and morphological properties of these compounds and polymers were characterized using FT-IR, ^{1}H-NMR, FESEM, and TEM. Using the weight loss method and electrochemical techniques (Tafel curves), the corrosion inhibition of modified polymers, blended polymers, and nanocomposites in 0.1 M hydrochloric acid on mild steel was investigated. The nanocomposites showed superior inhibition efficiency compared to the modified CS, blended polymer (modified CS/CMC). The presence of nanoparticles in the nanocomposites is responsible for their higher inhibition efficiency when compared to the

blended and modified polymers, yielding the following efficiency sequence: [modified CS/CMC/AgNPs [12] > modified CS/CMC/ZnONPs [13] > modified CS/CMC/CuONPs[11] > modified CS/CMC [7].The reason for the improved inhibition efficiency with increasing inhibitor concentration. The presence of multiple electron-donating groups (such as O, S, N, -COOH, and -OH) facilitates the formation of strong coordination bonds with the iron surface and nanoparticles. This increases the surface coverage of the chitosan (CS) particles on the metal across various concentrations and temperatures.

CONFLICT OF INTEREST

The authors declare that there is no conflict of interests regarding the publication of this manuscript.

REFERENCES

1. Khudhair NA, Bader AT, Ali MI, Husseini M. Synthesis, identification and experimental studies for carbon steel corrosion in hydrochloric acid solution for polyimide derivatives. AIP Conference Proceedings: AIP Publishing; 2020. p. 030014.
2. Ali MI, Khudhair NA, Huseeni MD, Kadhim MM, Khadom AA. Electrochemical Polymerization of New Schiff Base Monomer as an Anti-corrosion Coating on Carbon Steel in Saline Water: Experimental and Theoretical Studies. Journal of Bio- and Tribo-Corrosion. 2023;9(3).
3. Al-Turkustani AM. Thermodynamic, chemical and electrochemical investigation of pandanus tectorius extract as corrosion inhibitor for steel in sulfuric acid solutions. European Journal of Chemistry. 2013;4(3):303-310.
4. Mohammed MT, Al-Sieadi WN, Al-jeilawi OHR. Corrosion inhibitor of carbon steel in 3.5%NaCl solution with Schiff base compounds. International journal of health sciences. 2022:57-75.
5. Vincent Onuegu I, Wan Mohd Norsani Wan N, Mohammad Fakhratul Ridwan Z, Walid D, Mohd Sabri Mohd G, Richard Victor J. Corrosion inhibition of acid pickling –descaling-cleaning action on mild steel using aqueous hydroxyethyl cellulose. International Journal of Frontiers in Engineering and Technology Research. 2024;6(2):045-053.
6. Lu Y, Feng H, Xia H, Xia WH. Carboxymethyl Cellulose -Polyaniline Composites as Efficient Corrosion Inhibitor for Q235 Steel in 1 M HCl solution. International Journal of Electrochemical Science. 2022;17(11):221180.
7. Umoren PS, Kavaz D, Umoren SA. Corrosion Inhibition Evaluation of Chitosan–CuO Nanocomposite for Carbon Steel in 5% HCl Solution and Effect of KI Addition. Sustainability. 2022;14(13):7981.
8. Yin Q, Liu J, Zhong Z, Zhang Y, Zhang F, Wang M. Synthesis of phytic acid-modified chitosan and the research of the corrosion inhibition and antibacterial properties. Int J Biol Macromol. 2023;253:126905.
9. Farag AA, Al-Shomar SM, Abdelshafi NS. Eco-friendly modified chitosan as corrosion inhibitor for carbon steel in acidic medium: Experimental and in-depth theoretical approaches. Int J Biol Macromol. 2024;279:135408.
10. ElDesouky M, Eldougdoug W, Fouad E, Abd El-Moneim M. The synthesis of new corrosion inhibitors based on modified chitosan to provide protection over mild steel. Egyptian Journal of Chemistry. 2023;0(0):0-0.
11. Saleh MGA, Alfakeer M, Felaly RN, Al-Juaid SS, Soliman KA, Abd El Wanees S. Modified chitosan as an effective inhibitor against the corrosion of C-steel in HCl solutions. J Adhes Sci Technol. 2024;39(6):837-868.
12. Dai L, Wang X, Zhang J, Li C. Application of Chitosan and Its Derivatives in Postharvest Coating Preservation of Fruits. Foods. 2025;14(8):1318.
13. Martingo M, Baptista-Silva S, Mesquita R, Ferreira JP, Borges S, Pintado M. Exploring the potential of mealworm chitosan for hemodialysis applications. Sustainable Chemistry and Pharmacy. 2025;45:102013.
14. Žigrayová D, Mikušová V, Mikuš P. Advances in Chitosan Derivatives: Preparation, Properties and Applications in Pharmacy and Medicine. Gels. 2024;10(11):701.
15. Hamdi M, Sun H, Pan L, Wang D, Sun M, Zeng Z, et al. Chitosan and its derivatives as potential biomaterials for biomedical and pharmaceutical applications: A comprehensive review on green extraction approaches, recent progresses, and perspectives. Eur Polym J. 2025;229:113882.
16. Cheraghi E, Cheraghi Z. Chitosan: A Comprehensive Review of Structural Properties, Biological Activities, and Multidisciplinary Applications. Curr Trends Biotechnol Pharm. 2025;19(2):2372-2385.
17. Pereira Parchen G, Quaillet M, Alves de Freitas R, Hillaireau H. Chitosan-based nano-objects for drug delivery: a review of their chemical modifications, supramolecular organization and biological fate. RSC Pharmaceutics. 2025;2(6):1292-1322.
18. Akdaşçi E, Duman H, Eker F, Bechelany M, Karav S. Chitosan and Its Nanoparticles: A Multifaceted Approach to Antibacterial Applications. Nanomaterials. 2025;15(2):126.
19. Ruwaidah SS, Widad Abed S, El-Sayed N. Synthesis and Study Medical Application of Nanocomposites Based on grafted Chitosan /Polyvinyl alcohol. Ibn AL-Haitham Journal For Pure and Applied Sciences. 2024;37(1):236-250.
20. Huang L, Liu J, Wan L, Li B, Wang X, Kang S, et al. Comparative Study of Corrosion Inhibition Properties of Q345 Steel by Chitosan MOF and Chitosan Schiff Base. Materials. 2025;18(13):3031.
21. Kumar D, Khullar P, Jain V, Prakash R, Rai B. Investigating the corrosion inhibition mechanism of chitosan for steels in acidic environments: Experimental and computational studies. J Mol Struct. 2025;1337:142057.
22. Hefni HHH. Functional chitosan surfactants for corrosion inhibition in petroleum industry. Int J Biol Macromol. 2024;278:134704.
23. Cheng S, Shao Y, Chen M, Wang C, Zhu X, Zhang X, et al. Facile Fabrication of Attapulgite-Modified Chitosan Composite Aerogels with Enhanced Mechanical Strength and Flame Retardancy for Thermal Insulation. Polymers. 2025;18(1):98.
24. Akhlaq M, Uroos M. Evaluating the Impact of Cellulose Extraction via Traditional and Ionosolv Pretreatments from Domestic Matchstick Waste on the Properties of Carboxymethyl Cellulose. ACS Omega. 2023;8(9):8722-8731.
25. Liu S, Li H, Li X, Wang W, Rong C, Yang M, et al. PVA-enhanced green synthesis of CMC-based lithium adsorption films. Carbohydr Polym. 2025;349:122973.
26. Salem SS, Hashem AH, Sallam A-AM, Doghish AS, Al-Askar AA, Arishi AA, et al. Synthesis of Silver Nanocomposite Based on Carboxymethyl Cellulose: Antibacterial, Antifungal and Anticancer Activities. Polymers. 2022;14(16):3352.

27. Mohamad Zulkifli NAS, Ng K, Ang BC, Muhamad F. Fabrication of water-stable soy protein isolate (SPI)/ carboxymethyl cellulose (CMC) scaffold sourced from oil palm empty fruit bunch (OPEFB) for bone tissue engineering. Industrial Crops and Products. 2025;224:120325.
28. Yassin AY, Abdelghany AM, Salama RS, Tarabiah AE. Structural, Optical and Antibacterial Activity Studies on CMC/PVA Blend Filled with Three Different Types of Green Synthesized ZnO Nanoparticles. Journal of Inorganic and Organometallic Polymers and Materials. 2023;33(7):1855-1867.
29. El-naggar AM, Alsulaymani LA, Kamal AM, Albassam AA, Lakshminarayana G, Mohamed MB. Polyvinyl alcohol/ carboxymethyl cellulose blended polymers doped with PPy/ milled MWCNTs filler for Flexible optoelectronic and Energy Storage Applications. Polym Test. 2024;138:108551.
30. Pourmadadi M, Rahmani E, Shamsabadipour A, Samadi A, Esmaeili J, Arshad R, et al. Novel carboxymethyl cellulose based nanocomposite: A promising biomaterial for biomedical applications. Process Biochem. 2023;130:211-226.
31. Akhlaq M, Maqsood H, Uroos M, Iqbal A. A Comparative Study of Different Methods for Cellulose Extraction from Lignocellulosic Wastes and Conversion into Carboxymethyl Cellulose. ChemistrySelect. 2022;7(29).
32. Ndruru STCL, Marlina A, Nugroho BS, Pramono E, Sabrina Q, Yulianti E, et al. Preparation and characterization of polymer blend electrolyte membranes based on lithium acetate-complexed carboxymethyl cellulose (CMC) and carboxymethyl chitosan (CMCh) blend. Polymer Engineering and Science. 2023;64(2):761-778.
33. Elsayed Mahmoud D, Billa N. Physicochemical modifications in microwave-irradiated chitosan: biopharmaceutical and medical applications. J Biomater Sci Polym Ed. 2024;35(6):898-915.
34. Kruczkowska W, Kłosiński KK, Grabowska KH, Gałęziewska J, Gromek P, Kciuk M, et al. Medical Applications and Cellular Mechanisms of Action of Carboxymethyl Chitosan Hydrogels. Molecules. 2024;29(18):4360.
35. Li L, Baig MI, de Vos WM, Lindhoud S. Preparation of Sodium Carboxymethyl Cellulose–Chitosan Complex Membranes through Sustainable Aqueous Phase Separation. ACS Applied Polymer Materials. 2023;5(3):1810-1818.
36. Yan Q, Wei P, Peng R, Tian S, Li D, Tong Y, et al. Controllable Synthesis of Carboxymethyl Cellulose and Its Application in Tobacco Sheets. Wuhan Univ J Nat Sci. 2023;28(4):341-350.
37. Pal K, Banthia AK, Majumdar DK. Development of carboxymethyl cellulose acrylate for various biomedical applications. Biomedical Materials. 2006;1(2):85-91.
38. Kaur P, Alam T, Singh H, Jain J, Singh G, Broadway AA. Organic Acids Modified Starch–CMC Based Biodegradable Film: Antibacterial Activity, Morphological, Structural, Thermal, and Crystalline Properties. Journal of Pure and Applied Microbiology. 2023;17(1):241-257.
39. Anaya-Mancipe JM, da Silva VF, Becerra-Lovera AY, Dias ML, Thiré RMSM. Spinnability and Morphological Stability of Carboxymethyl Cellulose and Poly(Vinyl Alcohol) Blends by Electrospinning. Processes. 2024;12(12):2759.
40. Jiang ZN, Duan JM, Zeng XQ, Peng SY, Li YR, Xiong W, et al. Dramatic improvement in corrosion inhibition effect of carboxymethyl cellulose by modified with levodopa: Experimental study and first-principles calculations. Corros Sci. 2024;232:112037.
41. Gouda M, Khalaf MM, Al-Shuaibi MAA, Mohamed IMA, Shalabi K, El-Shishtawy RM, et al. Facile Synthesis and Characterization of CeO2-Nanoparticle-Loaded Carboxymethyl Cellulose as Efficient Protective Films for Mild Steel: A Comparative Study of Experiential and Computational Findings. Polymers. 2022;14(15):3078.
42. Zhang H, Zhao Y, Xu Z, Xu T, Wang J. Corrosion inhibition studies of carboxymethyl dextran: Experiments, quantum chemical calculations, and molecular dynamics simulations. J Mol Liq. 2025;419:126731.
43. Capacchione C, Partschefeld S, Osburg A, Gliubizzi R, Gaeta C. Modified Carboxymethylcellulose-Based Scaffolds as New Potential Ecofriendly Superplasticizers with a Retardant Effect for Mortar: From the Synthesis to the Application. Materials. 2021;14(13):3569.
44. Yousif E, Bakir E, Salimon J, Salih N. Evaluation of Schiff bases of 2,5-dimercapto-1,3,4-thiadiazole as photostabilizer for poly(methyl methacrylate). Journal of Saudi Chemical Society. 2012;16(3):279-285.
45. Saeed RS, Kawther Ayad O. Modified Polyvinyl Alcohol Containing New Imides / Iron Oxide Nanoparticles :Synthesis , Characterization and Biological Evaluation. Iraqi Journal of Pharmaceutical Sciences. 2025;34(2):60-75.
46. Ali A, Allehibi K, Al-Juboori N. Glycemic status in patients with primary hypothyroidism and its relation to disease severity. Mustansiriya Medical Journal. 2020;19(1):20.
47. Wang W, Meng Q, Li Q, Liu J, Zhou M, Jin Z, et al. Chitosan Derivatives and Their Application in Biomedicine. Int J Mol Sci. 2020;21(2):487.
48. Synthesis, Characterization, Study the Toxicity and Anticancer Activity of N,O-Chitosan Derivatives. International Journal of Pharmaceutical Research. 2020;12(02).
49. Shah SA, Sohail M, Karperien M, Johnbosco C, Mahmood A, Kousar M. Chitosan and carboxymethyl cellulose-based 3D multifunctional bioactive hydrogels loaded with nano-curcumin for synergistic diabetic wound repair. Int J Biol Macromol. 2023;227:1203-1220.
50. Saeed RS, Attiya HG, Obead KA. Synthesis and Characterization of Grafted Chitosan Blending with Polyvinyl alcohol / Nanocomposite and Study Biological Activity. Baghdad Science Journal. 2023.
51. Wang Y, Gao X, Qiu J, He W, Ma H. Enhanced anti-corrosion performance of sodium carboxymethyl cellulose coating on 5052 aluminium alloy via rapid gelation by metal ions. Colloids Surf Physicochem Eng Aspects. 2025;709:136145.
52. Suprianti L, Dwi Hery A, Sukamto, Khafid Ubay I, Ellyn Evina Ellys S. Corrosion Inhibition of Carbon Steel Using Chitosan as an inhibitor in 3.5% NaCl Medium. International Journal of Eco-Innovation in Science and Engineering. 2020;1(02):20-25.
53. Mixed-1,10-phenanthroline with Mn(II), Cu(II),Co(II), Hg(II) and Ni(II) complexes Synthesis, Antimicrobial Activity and Spectroscopic Characterization of Binuclear Schiff Base. International Journal of Science and Research (IJSR). 2016;5(5):1756-1763.
54. Messina E, Giuliani C, Pascucci M, Riccucci C, Staccioli MP, Albini M, et al. Synergistic Inhibition Effect of Chitosan and L-Cysteine for the Protection of Copper-Based Alloys against Atmospheric Chloride-Induced Indoor Corrosion. Int J Mol Sci. 2021;22(19):10321.
55. Aguilar-Ruiz A, Dévora-Isiordia G, Sánchez-Duarte R, Villegas-Peralta Y, Orozco-Carmona V, Álvarez-Sánchez J. Chitosan-Based Sustainable Coatings for Corrosion Inhibition of Aluminum in Seawater. Coatings. 2023;13(9):1615.
56. Attiya HG, Saeed RS, Abdulrada NJ, Jamur JMS, Majeed IY. Synthesis, Thermal Analysis and Corrosion Inhibition Study of Modified Polyvinyl Alcohol / Carboxymethyl Cellulose / AuNPs, AgNPs. ChemChemTech. 2026;69(5):90-99.